EFFECT OF NANO-SILICA (SiO₂) ON THE HYDRATION KINETICS OF CEMENT

Taher Abu-Lebdeh[1] – Relly Victoria V. Petrescu[2] – Moayyad Al-Nasra[3] – Florian Ion T. Petrescu[4*]

[1]Department of Civil, Architectural and Environmental Engineering, North Carolina A&T State University, Greensboro, USA
[2]Transport Traffic and Logistics department, Bucharest Polytechnic University, Bucharest 060042 (CE) Romania
[3]Department of Civil and Infrastructure Engineering, American University of Ras Al Khaimah, AURAK, Ras Al Khaimah, UAE
[4]Theory of Mechanisms and Robots department, Bucharest Polytechnic University, Bucharest 060042 (CE) Romania

Abstract:

This study investigated the influence of adding nano silica (SiO2) on the cement hydration process, particularly on the formation of calcium silicate hydrate (C-S-H) at different stages of hydration. The study investigated the effect of adding nano-silica on the mechanical properties of the hardened cement corresponding to the formation of C-S-H during the hydration process of a cement paste. Specimens made up of four different percentage of nano silica (0%, 1%, 3% and 5%) were tested at different stages of hydration ranging from 3 to 56 days. The effect of nano-silica on the compressive strength, stress-strain, and elastic modulus of nano-cement was examined using MTS and Forney testing machines. The signature phase and formation of C-S-H and calcium hydroxide (CH) were monitored using Fourier Transform Infrared Spectroscopy (FTIR) and Scanning Electron Microscopy (SEM). The study also investigated the effect of curing method (vacuum and water curing) on the strength development. The experimental results show that the formation of calcium silicate hydrate (C-S-H) increases significantly during the early stages of hydration which correspond to the drastic increase in compressive strength. The formation of C-S-H continues to increase throughout the 56 days but at a moderate rate. The results reveal that 1% of nano silica by volume of cement is the optimum ratio that yields the maximum strength. The results also indicated that the strength of the traditional water cured specimens were higher than that of vacuum cured specimens.

---

* Corresponding author.

1 Introduction

The hydration of cement paste is generally responsible for the development of essentially every engineering property of cement paste. Cement is manufactured by the crushing, milling, and proper proportioning of lime, silica, alumina, iron, and gypsum. When cement is in the anhydrous state, four main types of minerals exist: (1) alite (C3S) which is a compound that hydrates and hardens at an accelerated rate. It is largely responsible for the initial setting and early strength of the cement paste. (2) belite (C2S) is a compound that hydrates and hardens at a slow rate. It is largely responsible for the cement paste's strength gained after one week of hardening. (3) The tricalcium aluminate (C3A) doesn't contribute much to the strength of the cement paste. However, it liberates a lot of the heat during the beginning stages of hydration. (4) Tetracalcium Aluminoferrite (C4AF) is a compound which doesn't affect the cement paste's strength much. It acts as a fluxing agent which reduces the melting temperature of the raw materials within the kiln [1]. Other chemicals that may exist are: sodium oxide (Na2O), potassium oxide (K2O) and gypsum (CSH2). From the hydration process of cement, several products are formed: calcium silicate hydrate, calcium hydroxide, calcium aluminates and calcium sulfoaluminates. During the hydration process of cement, the tricalcium aluminate reacts with the gypsum to produce ettringite and heat. Next, the tricalcium silicate hydrates to produce the calcium silicate hydrates, lime, and heat. The calcium silicate hydrates generate strength during this phase within the cement paste. This process has a very slow rate; however, this compound produces the long-term strength of concrete. Calcium Silicate Hydrate (CSH) is the main and most important constituent of cement paste. It's its hydration forms most of the new solid phases that give hardened cement paste its strength. It occupies approximately 50% of the paste volume and responds to nearly all the engineering properties of the cement paste. Calcium hydroxide (CH) occupies approximately 15% of the cement paste by volume. CH forms as crystals within the cement paste that nucleate in the capillary pores and are large enough to be seen under an optical microscope.

Additives may affect the hydration kinetics of cement. Fly ash, for instance, contains pozzolans and consumes CH in the pozzolanic reaction. Zhang found that less CH would decelerate the hydration reaction. The higher the fly ash content, inversely the CH content is reduced [2]. The silica fume additive also contains pozzolans, and the presence of silica fume increases the rate of cement hydration during the early stages of hydration. Bagheri and co-researchers [3] show that the addition of 5% silica fume and 15% of fly-ash provide a remarkable improvement in the early and late ages. They concluded that the acceleration rate increases, as the particle fineness increases due to surface nucleation. They found that the optimum silica fume content is about 5% and a further increase doesn't result in further improvement in concrete properties. Björnström and co-researchers have studied the effect of adding nano-silica on the hydration process of C3S pastes. They investigated: phase dissolution of C3S, silica polymerization, calcium–silicate–hydrate (C–S–H) gel formation, and bulk properties of the hardening paste. They show that the accelerated effect was very clear when the concentration of nano-silica increased from 1% up to 5%. However, 1% of the material seems to have remarkable effects. The DR-FTIR was used in their study to monitor all phases [4]. Jonbi and his co-researchers investigated the use of nano-silica in improving compressive strength and durability of concrete. They replaced cement with nano-silica by weight of 3%, 5%, 10%, and 15%, along with superplasticizer. Their result indicated that the best improvement in 28 days compressive strength was with 5% nano-silica. They showed a small decline in compressive strength with 10% nano-silica while there was a significant decrease of compressive strength with 15% nano-silica [5]. Sobolev and others studied polycarboxylic mixed with nano-silica to improve workability and strength of self-compacted concrete "SCC". Their results indicated an increase in compressive strength of the concretes modified with nano particles. They concluded that the effective dispersion of nano particles is an important factor to obtain better performance of composite materials [6]. Maheswaran and his colleagues have shown that including nano-silica in cement paste will improve its physical and chemical properties. They indicated that the reaction of nano-silica with excess CH during cement hydration has led to a reduction in calcium hydroxide content, thus resulted in a reduction in chemical leaching of CH and sulfate attack. Also, they observed that the addition of nano-silica in normal strength mortar increased the compressive strength, and early hydration of cement mortar which is attributed to pozzolanic nature of nano-silica [7]. Ye Qing and other researchers reported that the compressive strength increases with the increase in replacement percentage. Their experiments used an

addition of 0%, 1%, 2%, 3%, and 5% of nano-silica to cement replacement by weight [8]. Their results show great improvement in compressive strength at all ages of testing. Signifying 5% of cement replacement was optimum. Cheuny and his co-researchers concluded that using admixtures such as water reducing or plasticizing admixture with nano-silica decreases the agglomeration and directly impacts kinetics of hydration, resulting in powerful dispersing capability, and led to improvement in workability as well as durability and concrete strength through the increase in the the formation of silicate calcium hydrate [9].

In an effort to better comprehend the mechanisms underlying cement hydration, the use of new technology is needed to enhance the prediction of properties. The chemistry behind cement hydration is commonly studied using spectroscopic methods. This present work investigates the mechanical properties of cement paste as it goes through several stages of hydration, monitored by SEM (Scanning Electron Microscopy) and FTIR (Fourier Transform Infrared Spectroscopy).

2   Materials and Methods

The objective of this experimental study is to investigate the effect of nano-silica on the cement hydration and on the mechanical properties of cement paste. Approximately 211 specimens of 4 in. by 8 in. (10.2 cm by 20.3 cm) cylinders and 2 in. 5.08 cm) cubes were prepared and cured in water and in vacuum for 3, 7, 14, 28, and 56 days prior testing. Compressive strength testing was carried out using the Forney Universal Testing Machine and MTS Landmark Servo Hydraulic Testing System (MTS). The Fourier Transfer Infrared Spectroscopy (FTIR) and Scanning Electron Microscope (SEM) were used to monitor the chemical transformations of the cement paste during different stages of hydration.

Portland cement Type 1 and nano silica (15-20 nm in size and consists of >99% pure silica) were utilized as the cementitious materials in this study. The polycarboxylate superplasticizer used herein is a high-performance acrylic based polymer. It's specifically designed to improve the strength, modulus of elasticity, durability, workability, and flexibility of concrete properties. It is an effective dispersant and high range water reducer (HRWR).

Four {4} mix designs were created: M1, M2, M3, and M4, consisted of a control (0%), 1%, 3%, and 5% by volume of cement replaced with nano-silica, respectively. The water to cement (w/c) ratio was

0.27 using polycarboxylate superplasticizer. The superplasticizer was kept constant at 2.31% by weight of water. 111 cubes and 100 cylinders were prepared, totalling to 211 specimens.. Half of the specimens were cured in lime water, while the other half were encased in vacuum seal bags with the air vacuumed out from the bags (vacuum curing). After curing for 3, 7, 14, 28, and 56 days, hardened specimens were tested for compressive strength, SEM, and FTIR testing.

Four different testing machines were used in this experimental study. The compression test was carried out using the Material Test System (MTS). The MTS 810 Landmark Servohydraulic system is used herein for cube compression. It includes MTS software, FlexTest controls, and MTS servo-hydraulic technology. The Forney Universal Testing Machine was used to carry out the cylinders testing.

The machine has a 400 kip load capacity and a load rate of 12,000 lbs/min. The SEM EVO LS (Scanning Electron Microscope) was used to obtain images for possible C-S-H formation.

The SEM EVO LS is a device made by ZEISS, used herein to study the microstructure and analysis the hardened cement paste specimens. EVO LS has an environmental mode that can capture nano scale interactions within the hardened cement samples under different temperatures, pressures, and humidities. It should be noted that the EVO LS system includes EVO HD which can increase both the image resolution and contrast. The FTIR (Fourier Transform Infrared Spectroscopy) was used to monitor the formation of C-S-H throughout the 56 testing days. The Thermo Scientific Nicolet iS10 FT-IR Spectrometer was used to examine the chemical properties within the hardened cement paste throughout the hydration process.

The compression tests were conducted following ASTM C109 - 16a [10]: Standard Test Method for Compressive Strength of Hydraulic Cement Mortars (Using 2-in. or [50-mm] Cube Specimens) and ASTM C39 - 17a [11]: Standard Test Method for Compressive Strength of Cylindrical Concrete Specimens. After mixing, 4x8 cylinders and 2-in cubes specimens were prepared in accordance with the ASTM standard specifications. All cylinders and cubes were de-molded after 24 hours and then cured for 3, 7, 14, 28, and 56 days before testing. Two curing methods were used, water and vacuum. Water curing involved the standard placement of the specimens into a water tank, while the vacuum curing consisted of encasing the specimens in vacuum seal bags which remained completely sealed until the age

of testing. After curing, the specimens were dried in air for approximately one hour before testing. The MTS machine was used to carry-out the compression tests for 2 in. cube specimens.

The load rate for the MTS machine was 0.01 in/s. The displayed data included displacement (inches), loading (pounds), and the time (seconds). The data was later transferred into Excel to calculate the stress and strain. Compression tests of 4x8 cylinders were conducted using the Forney testing machine.

The Forney machine tests were performed with a load rate of approximately 12,000 lbs/min. Cylinders were capped with either rubber pads or a capping compound in accordance to ASTM C-617. Forney captured the maximum peak load applied to each cylinder under testing.

Fourier Transform Infrared Spectroscopy or FTIR was conducted to monitor C-S-H growth during the hydration process. The Thermo Scientific Nicolet iS10 FT-IR Spectrometer was utilized to carry out the monitoring. It delivers the highest confidence in the verification and identification of materials. With the use of OMNIC software, the Nicolet iS10 can manage results and provide accurate and valid results. Several steps were followed to carry out FTIR testing. Step 1- sample preparation: The samples used for this study were fragments obtained from the crushing of the cylinder and cubes, succeeding the compressive tests. Step 2: perform a background check to remove traces of dissolved gases and solvent molecules. In this step, the background spectrum that contains information about the surrounding gases and solvent molecules was later subtracted from the spectrum obtained from the tested samples. It should be noted that the subtraction process is an automatic feature and process that happens whenever a new sample is tested. In step 3, and after the background has been collected, a sample prepared in step 1 was placed over the diamond of the device, and a single beam spectrum containing the absorption bands was collected. In this study, at least 5 spectrums were collected for each sample, and the average of all the spectrums collected was recorded and illustrated. In step 4, the data from the collected spectrum was analyzed using the OMNIC software. For each sample, the absorption frequency bands assigned to each sample spectrum were observed for normal modes of vibrations within the molecules. These spectrums were later analyzed and compared.

The testing procedures for the SEM were performed in several steps: At each testing age, one cylinder from each mix of the water and vacuum cured specimens was cored using a Milwaukee Coring Rig Dymodrill.

Segments of approximately ¾ inches in diameter and ¾ inches in depth were cutouts from the center of each cored sample using a diamond saw.

The segments were then labelled (percentage of nano silica, curing method, days of hydration or testing age, and an arrow directing to the bottom surface used for imaging). The segments were then prepared for SEM images. The preparation process includes applying an epoxy mixture, then placing the samples in a vacuum pump (set at 27 kPa until bubbles formed at the surface) for approximately nine hours until the epoxy mixture hardens. The segments were then sanded and polished using a MetaServ 250 grinder-polisher, followed by placing the samples in a container filled with ethanol and sonicated for 10 minutes before performing the microscopic examination.

3 Results

3.1 Compressive strength

As aforementioned, a compressive strength of 2-in cubes of hardened cement paste was conducting using the MTS testing machine. Results of 3 cubes of each percentage of nano silica at each testing age and for each curing method were averaged and tabulated in Table 1. Similarly, the resulted stress-strain curves of the averaged 3 specimens were determined for 0%, 1%, 3%, and 5% at each testing age of 3, 7, 14, 28, and 56 days for both water and vacuum curing methods. Samples of theses curves are illustrated in Figs. 1 and 2.

As mentioned earlier in the testing procedures section, the Forney universal testing machine was used to conduct compressive strength of cylindrical hardened cement paste specimens.

Fig. 3 illustrates the average compressive strength of 3 specimens for each percentage of nano silica tested at different hydration ages after water curing. As shown in the figure, the 1% and 3% nano silica specimens perform significantly higher than that of the controlled.

Fig. 4 shows the effect of the amount of nano silica on the compressive strength at different hydration stages. The figure also compares compressive strengths of the control specimens when cured in water and vacuum. Results indicated that the cylinders cured in water have higher compressive strength than that cured in the vacuum.
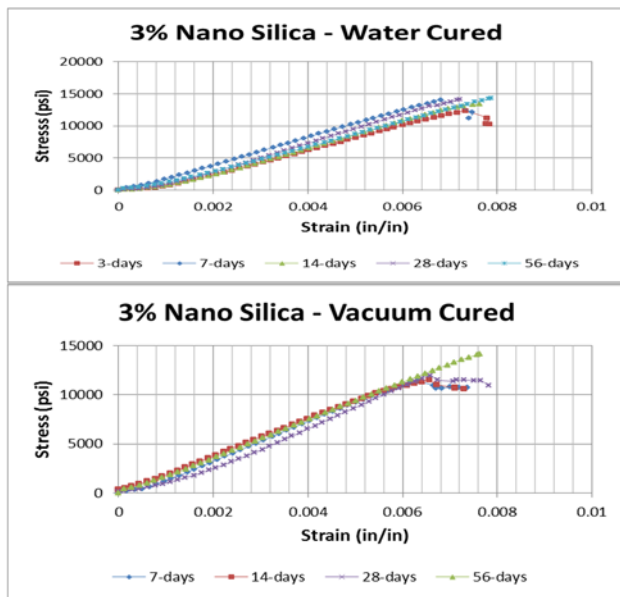
Figure 1. Stress-strain curves of 3% nano silica: (a) water cured and (b) vacuum cured samples. [1 Mpa = 145 psi; 1 in.= 25.4 mm].
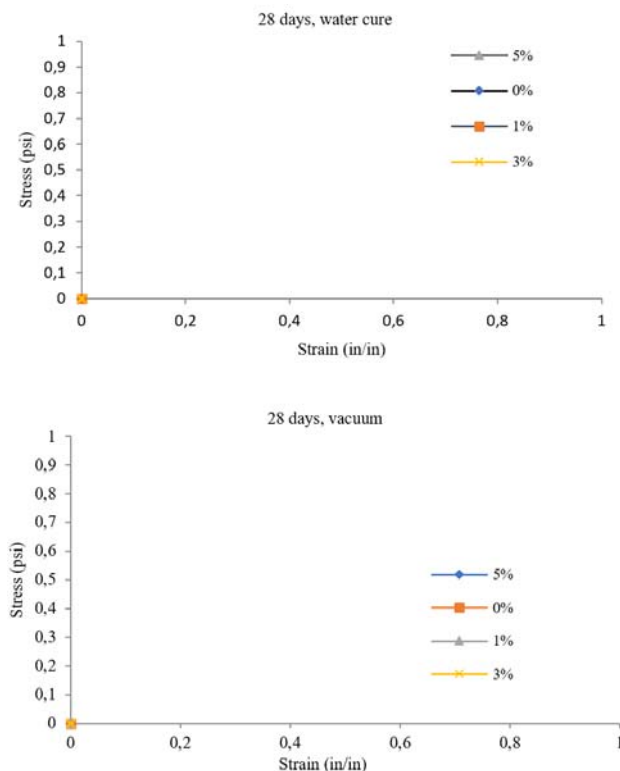

Figure 2. Stress-Strain curves of different percentage of nano-silica at 28 days of (a) water cured and (b) vacuum cured specimens. [1 Mpa = 145 psi; 1 in.= 25.4 mm].

Table 1. Compressive strength (psi) of 2-in hardened cement paste [1 Mpa = 145 psi]

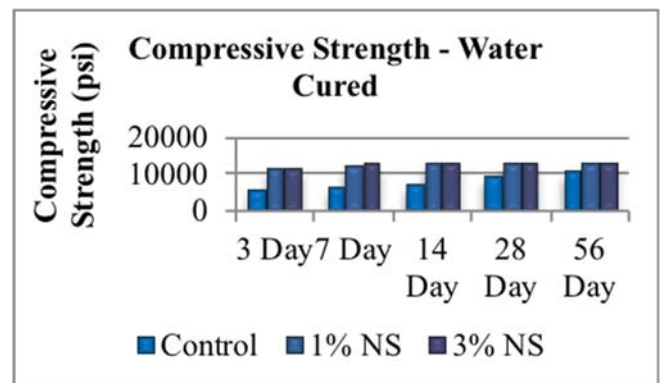|	Water Cured				
% N.S.	3	7	14	28	56
Control	6149	8377	8234	11921	12793
1%	12531	13450	14270	14377	14537
3%	12300	14042	13375	14174	14346
5%	11116	10710	7210	10788	11182
	Vacuum Cured				
	3	7	14	28	56
Control	5070	7542	7031	8526	12219
1%	-	13703	14154	14390	14354
3%	-	9810	11515	11515	14162
5%	-	9033	7559	12866	11972

Figure 3. Compressive strength of cylindrical specimens cured in water [1 Mpa = 145 psi; 1 in.= 25.4 mm].
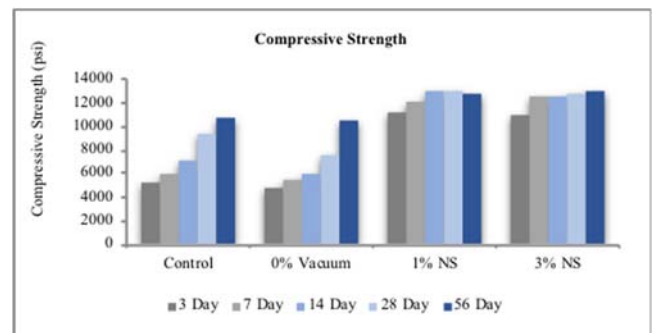

Figure 4. Effect of nano silica on the cylinder compressive strength. [1 Mpa = 145 psi].

3.2 The SEM results

The SEM-EVO LS was used to obtain microscopic images of the hardened cement paste hydrated at different ages. After obtaining the images, further

analysis, using MatLab, was conducted to filter the images using a Gaussian filter, and to determine the percentages of chemical products for which that images portray.

The MatLab was also used to generate histograms outlying the major constituents of the hydrated cement. From the gray level imaging, four main phases can be identified: porosity (P), calcium hydroxide (CH), calcium silicate hydrate (C-S-H), and unhydrated products (UP). In this study, the following phases were assigned with the specified color: P – Blue, C-S-H – Green, CH – Red.

Fig. 5(a) shows the original SEM image of hardening cement paste containing 1% nano silica and cured in water for 7 days.

Fig. 5(b), shows the same sample after filtered using the Gaussian filter. Features from this image are lighter and more distinguished. Fig. 5 (c) displays the color phases of the same sample and after filtering.

Fig. 6(a) shows the gray level histogram of the sample after filtered while Fig. 6(b) shows the histogram of the same sample with color phases and the percentage of each respected color phase. It should be noted that forty {40} specimens were analyzed for SEM and figures similar to figures 5 and 6 were generated for each case.
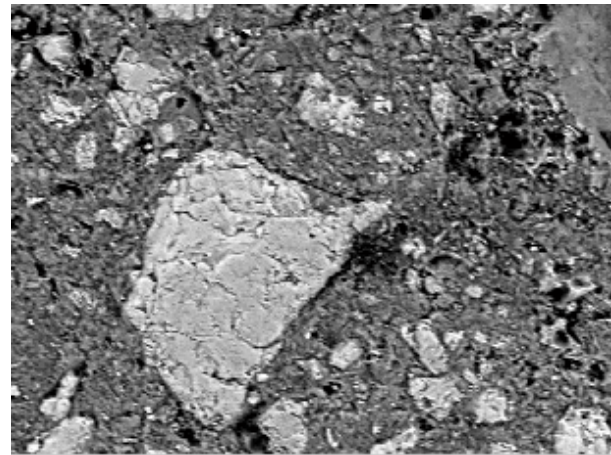
The SEM Results gathered from the MatLab analysis are tabulated in Tables 2 and 3. Table 2 shows the averages of porosity, calcium silicate hydrate, and calcium hydroxide of specimens containing 0%, 1%, 3%, and 5% of nano silica in cement paste cured in water for 3, 7, 14, 28, and 56 days. As shown, there is an increase in C-S-H formation as the hydration increases from 3 days to 56 days. This is true for each percentage of nano silica. The results also show that specimens of 5% nano silica produce the highest C-S-H formation. Similar results can be seen in Table 3 for specimens cured in a vacuum.
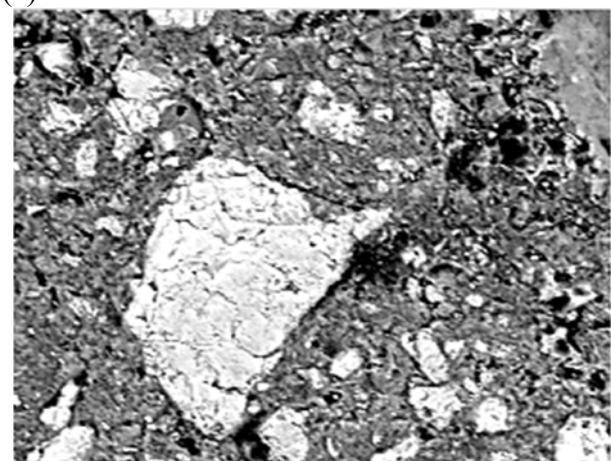
3.3 The FTIR results

The effect of adding nano silica on the formation of C-S-H was monitored for specimens tested at 3, 7, 28, and 56 days, by acquiring an FTIR spectrum for each specimen cured in water and vacuum. The process starts by acquiring the reference spectrum of the anhydrate dry cement as shown in Figure 7.

As seen, two major peaks occur around the wavelength numbers of 877 cm^{-1} and 1100 cm^{-1}. From the chemical composition of Portland cement, the peaks can possibly be assigned to the CaO and the SiO_2 respectively [12]. Second, the spectra for the hydrated 3, 7, 28, and 56 days water and vacuum
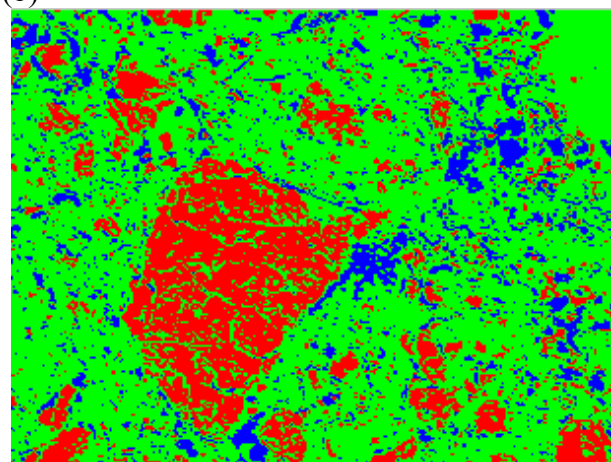
cured samples were recorded followed by the subtraction of the reference dry cement spectrum [13-28]. The purpose of the subtraction is to remove the bonds of the reference material away from that of the hydrated specimens.

(a)

(b)

(c)

Figure 5. Grey level SEM images: (a) Original, (b) filtered, (c) colored phases.

_____

the corresponding spectrum for all testing days. It should be noted that the spectra and the area of possible C-S-H for all specimens of different nano silica percentages, including vacuum curing were determine but not shown. Table 4 displays the area (amounts) of C-S-H formation from each case of hydration age, a percentage of nano silica replacement, and curing method.
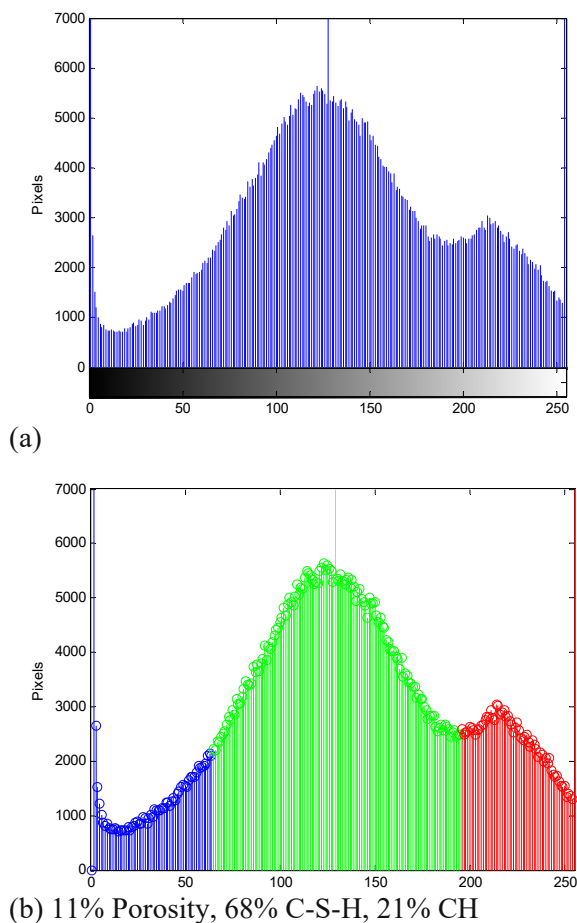

(a)

(b) 11% Porosity, 68% C-S-H, 21% CH

Figure 6. Grey level histogram: (a) filtered, (b) colored phases.

The subtraction was performed by determining the difference in absorbance between the two spectra and plotting the difference against the wavenumber. Figure 8 illustrates the resulted spectrums of the control specimens at all ages. The signatures of hydration can be seen within the 900 to 1200 cm-1 region. Also notice the large peak around 3400 cm-1, which can be associated with hydrogen bond (O-H) or capillary water within that region.

As the hydration process continues, more of the H2O molecules complement the production of C-S-H shown within the 900 to 1200 cm-1 region [4]. Knowing that the formation of C-S-H occurs within the approximate region of 900 to 1100 cm-1, spectra were zoomed into this area for further analysis. Using the OMNIC software, the area of the peak region associated with C-S-H can be exerted by creating a baseline between the two dips neighbouring that region. In Figure 9, the areas of the water cured control specimens were calculated and shaded with

Table 2. SEM Chemical Area - Water Cured

		Control	Nano Silica with Superplasticizer		
Days	Area	0%	1%	3%	5%
3	P	17	15	11	11
	C-S-H	59	65	76	79
	CH	24	20	13	10
7	P	11	11	10	5
	C-S-H	64	68	80	80
	CH	25	21	10	15
14	P	15	14	12	7
	C-S-H	66	74	82	84
	CH	19	12	6	9
28	P	17	13	8	3
	C-S-H	67	77	83	85
	CH	16	10	10	12
56	P	10	9	6	3
	C-S-H	70	81	85	86
	CH	20	10	9	11

Table 3. SEM Chemical Area - Vacuum Cured

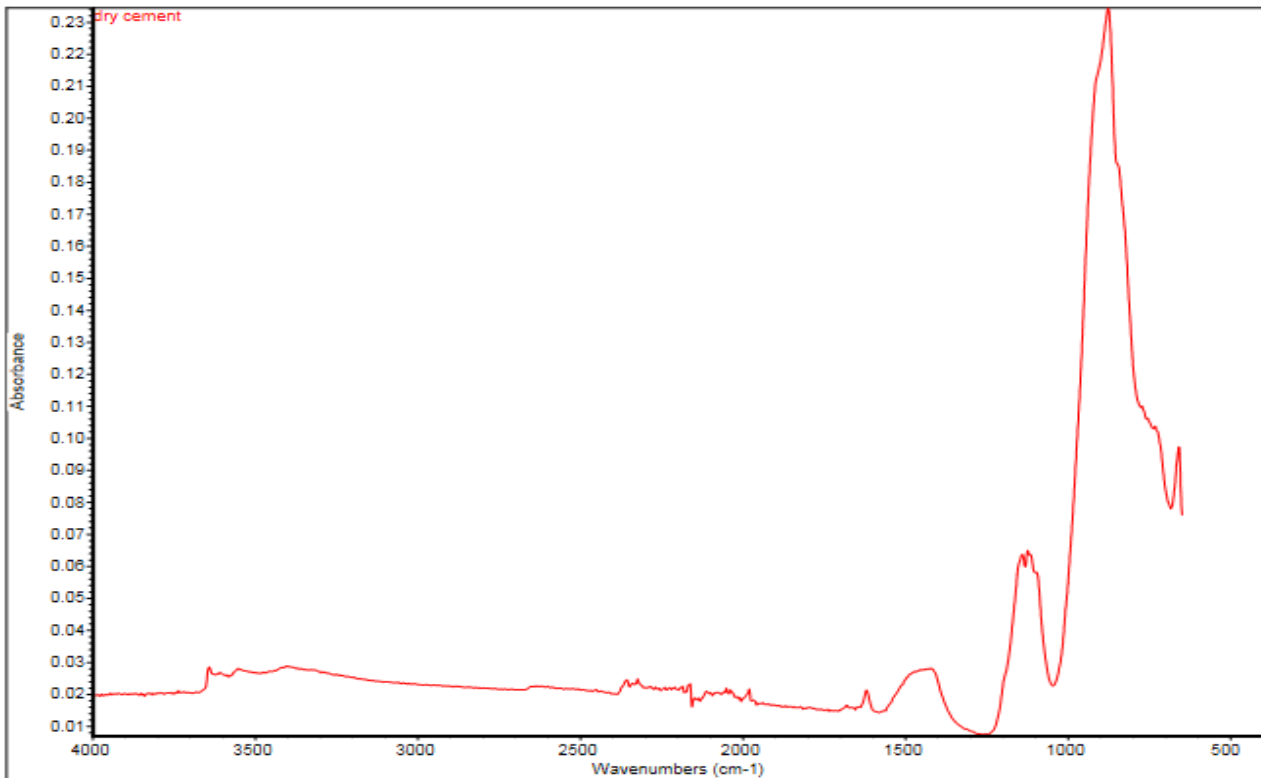|		Control	Nano Silica with Superplasticizer		
Days	Area	0%	1%	3%	5%
3	P	19	18	10	11
	C-S-H	61	67	74	77
	CH	20	15	16	12
7	P	12	10	10	8
	C-S-H	62	68	81	79
	CH	26	22	9	13
14	P	17	15	14	10
	C-S-H	67	72	74	79
	CH	16	13	12	11
28	P	15	8	8	11
	C-S-H	69	75	82	80
	CH	16	17	10	9
56	P	16	7	5	3
	C-S-H	70	83	85	86
	CH	14	10	10	11

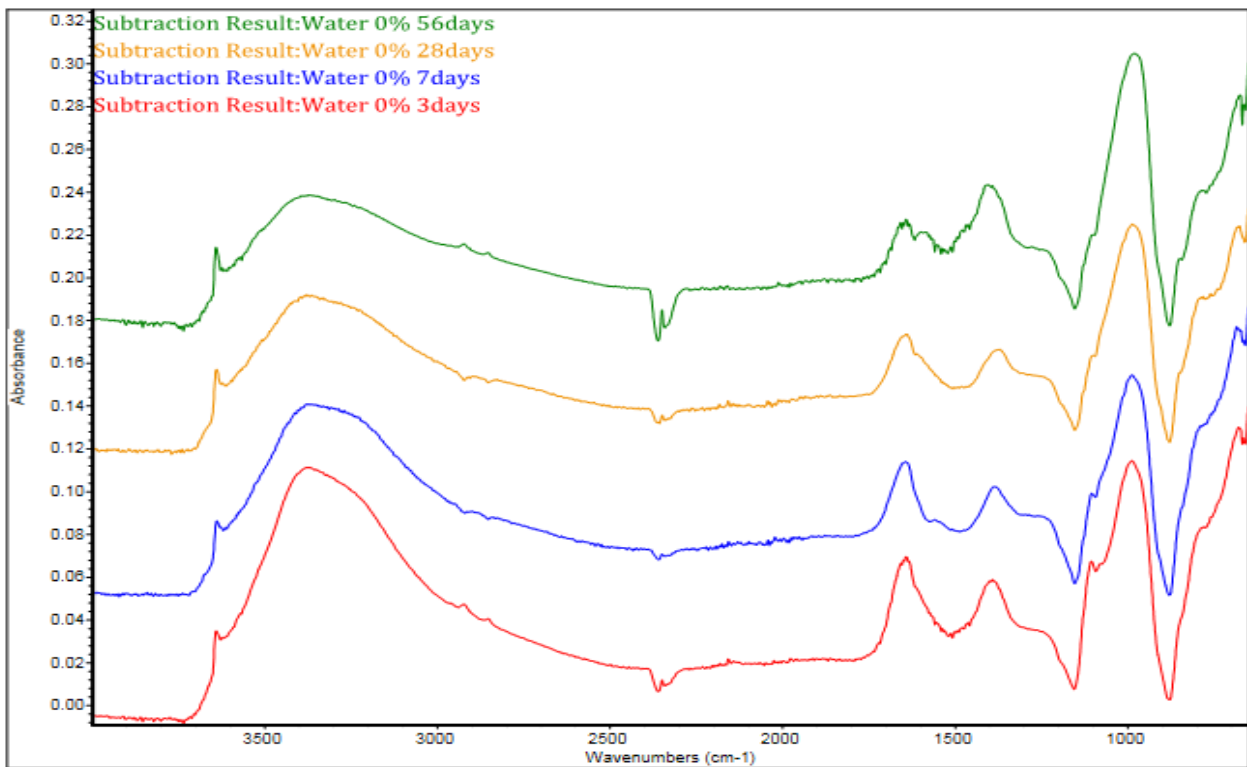*Figure 7. The spectrum of anhydrate dry cement.*

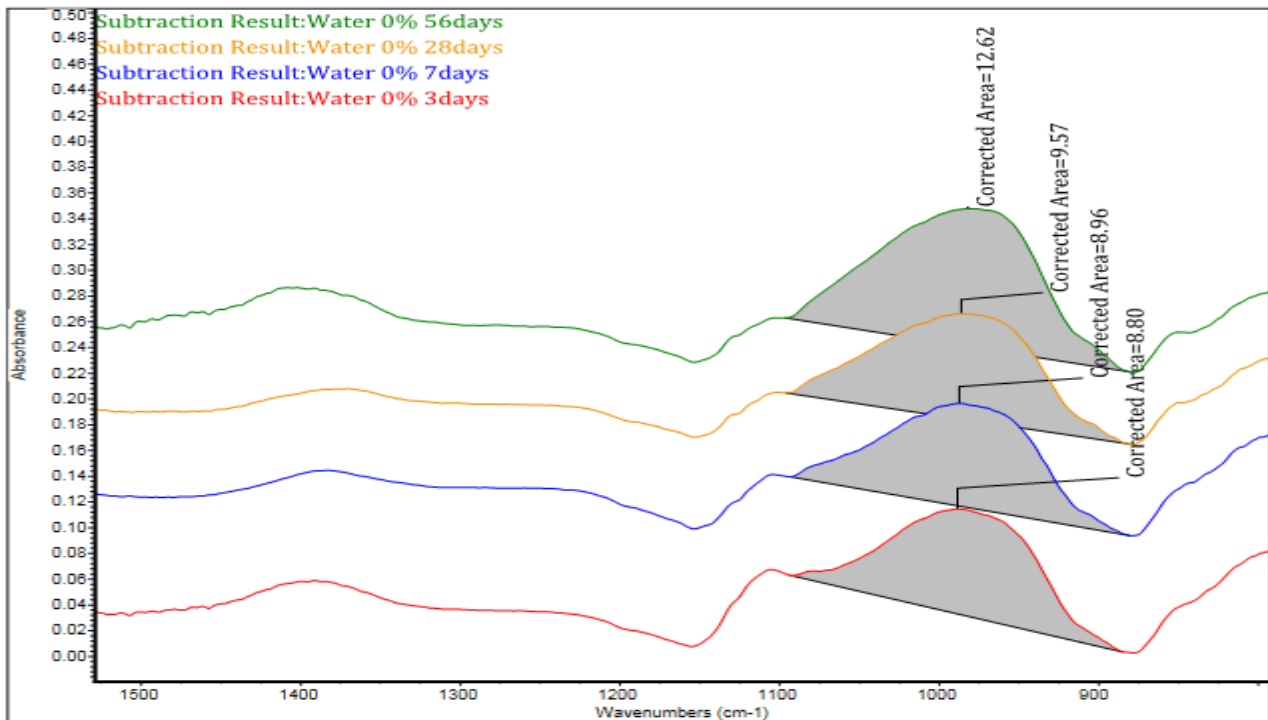*Figure 8. The FTIR results of the controlled specimen at different ages.*

Figure 9. Areas of possible C-S-H formation (800 - 1600 cm-1).

Table 4. Amount of C-S-H Formation

Area of C-S-H Region - Water Cured Specimens			
	Percentage of Nano Silica		
Days	Control	1%	3%	5%
3	8.8	7.12	5.59	7.06
7	8.96	9.52	6.15	8.21
28	9.57	10.47	7.31	8.26
56	12.62	11.57	9.56	10.44
Area of C-S-H Region - Vacuum Cured Specimens			
	Percentage of Nano Silica		
Days	Control	1%	3%	5%
3	9.9	-	-	-
7	10.2	7.55	9.14	5.69
28	11.18	9.56	9.31	6.41
56	11.91	12.23	11.32	7.32

4   Discussion

4.1. Compressive strength

The effect of nano silica on the compressive strength of hardened cement cubes is shown in Table 5. The table compares compressive strengths of specimens that incorporated nano silica to that with no nano silica added (control). The addition of NS resulted in an increase in compressive strength at all stages of testing.

As seen, a significant increase in strength can be noticed during the early ages, but the percentage of growth is not as significant as the hydration period increases to 56 days. However, the results still portray 12% - 20% increase in strength compared to the control. Comparing the percentage of nano silica, the 5% NS samples performed poorly in comparison to the 1% and 3%.

Table 5. Effect of nano silica on the compressive strength (cube specimens)

	Water Cured %				
N.S. Perc.	3	7	14	28	56
1%	104	61	73	21	14
3%	100	68	62	19	12
5%	81	28	-	-	-
	Vacuum Cured %				
	3	7	14	28	56
1%	-	82	101	69	18
3%	-	30	64	35	16
5%	-	20	8	51	-

_____

Table 6. Effect of NS on the Cylinders compressive strength

	3 Day	7 Day	14 Day	28 Day	56 Day
1% NS	116%	101%	84%	36%	19%
3% NS	112%	109%	78%	34%	20%

The results indicated that the 1% NS is the optimum percentage due to its consistent and higher compressive strengths at almost all testing ages. Regarding the curing methods, there is no significant difference in strength between the water and vacuum cured samples.

It should be noted that the results of the water cured cylindrical compressive strength in Table 6 confirm all findings of the cubes compressive strength (Table 5). Table 6 shows the percent increase in strength of the cylinders that incorporate NS in comparison to the control specimens.

4.2. SEM

The SEM images along with Matlab analysis were used to observe the essential features of each hydration phase and the way the transformation would look like. The SEM results indicated an increase in C-S-H formation throughout the hydrations stages. Comparison with the control specimens shows a significant increase in C-S-H formation due to the addition of nano silica. A greater increase in C-S-H formation was observed in specimens with 5% NS in comparison to the 1% and 3% NS. This finding should indicate a greater increase in compressive strength of the 5% NS specimens; however, the compressive strength results show that the 5% NS samples portrayed the lower strength values when compared to the 1% and 3% specimens. The reasoning behind the dissimilarities could be due to the area of which the SEM images data was gathered and collected to determine the amount of C-S-H or hydrated products. The SEM images only look into one location under 1300x magnification within a specific sample. Thus, the area examined under the SEM is a small representation of the sample, therefore provides an estimate of the full sample strength. It should be noted that the curing method did not affect the formation of C-S-H. This was obvious in the similarity in the C-S-H growth in specimens that were cured in water and vacuum.

4.3. FTIR

The FTIR was used, along with the omnic software to monitor the hydration process of modified Portland cement paste with 0%, 1%, 3%, and 5% nano silica hydrated between 3 to 56 days under the water curing and vacuum curing. The process examines the chemical properties of the hydrated cement paste and monitors the changes in mechanical properties as the reactions take place. Calcium Silicate Hydrate (C-S-H) is a weak bond structure which appears in the 900 - 1200 cm-1 region (around 1100 cm-1) and can be associated with the peak in that region. The appearance of this broad absorption at (900–1200 cm−1) is due to the polymeric silica and the formation of calcium silicate hydrate C-S-H. It is worth noting that the formation of the calcium silicate hydrate (C-S-H) is caused by the reaction of C3S (alite) which is responsible for the early strength, while the growth at (1500–1700 cm−1) is indicative of the formation of C-S-H due to the reaction of C2S (belite) which is responsible for the long-term strength development. Using the Infrared absorption spectroscopy, the amounts of C-S-H growth have been determined for each case of the study and reported in Table 4. The results indicated an increase in C-S-H formation with age. This is true for both water and vacuum curing. From the findings, it may be concluded that modified Portland cement paste with 1% nano silica represents the optimum case. Specimens with 1% NS exhibited the highest increase in C-S-H formation as shown in Table 4. This increase signifies the highest increase in compressive strength of the hardened cement as shown in Table 1 and Fig.4.

The hydration process can be examined by determining the change in the C-S-H area over the course of 56 days. Considering the differences in C-S-H areas between the hydration intervals and plotting the change in the area with respect to time, the rate of hydration can be determined. Figures 10 and 11 signify a decrease in hydration after 3 days, and from there the hydration tends to increase at a slow pace leading up to 56 days. The same occurrence takes place during the vacuum cured samples as well. Again, the modified cement paste with 1% NS shows superiority over the other percentage of nano silica.
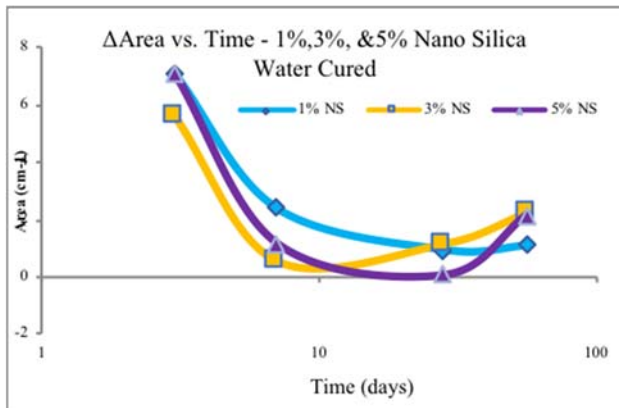
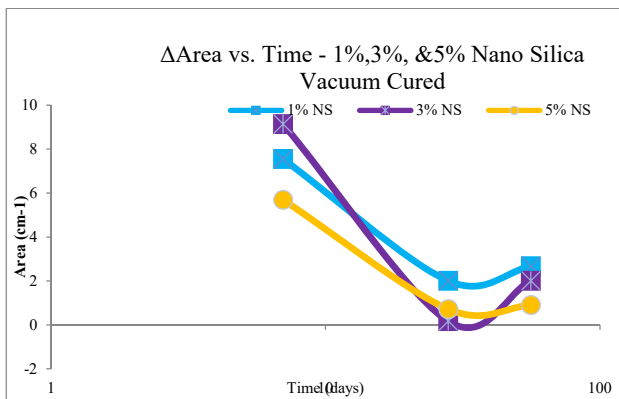*Figure 10. Change in area of C-S-H for water cured specimens.*

Figure 11. Change in area of C-S-H for vacuum cured specimens.

5 Conclusion

This study investigated the influence of adding nano silica (SiO2) on the cement hydration process, particularly on the formation of calcium silicate hydrate (C-S-H) at different stages of hydration. Because calcium silicate hydrate is the main hydration product and the main source of concrete strength, the study investigated the effect of adding nano-silica on the mechanical properties of the hardened cement corresponding to the formation of C-S-H during the hydration process of a cement paste. Specimens made up of four different percentage of nano silica (0%, 1%, 3% and 5%) were tested at different stages of hydration ranging from 3 to 56 days. The effect of nano-silica on the compressive strength, stress-strain, and elastic modulus of nano-cement was examined using the MTS and Forney testing machines. The signature phase and formation of C-S-H and calcium hydroxide (CH) were monitored using the Fourier Transform

Infrared Spectroscopy (FTIR) and Scanning Electron Microscopy (SEM). The study also investigated the effect of curing method (vacuum and water curing) on the strength development. The experimental results show that the formation of calcium silicate hydrate (C-S-H) increases significantly during the early stages of hydration which corresponds to the drastic increase in compressive strength. The formation of C-S-H continues to increase throughout 56 days, but at a moderate rate. The results reveal that 1% of nano silica by volume of cement is the optimum ratio that yields the maximum strength. This increase in strength may be attributed to the reaction between nano-silica and Calcium Hydroxide (CH) to develop more calcium silicate hydrate(C-S-H) resulting in higher strength. The results also indicated that the strength of the traditional water cured specimens were higher than that of vacuum cured specimens.

Several techniques have been employed to better understand the mechanisms underlying the hydration process of the modified Portland cement with nano silica. This study investigated the mechanical and chemical changes during the hydration stages of the cement paste. The work investigates the mechanical properties of the hardened modified cement paste as it goes through several stages of hydration, monitored by the SEM and FTIR. Calcium Silicate Hydrate (CSH) is the main and most important constituent of the cement paste. Its hydration forms most of the new solid phases that give hardened cement paste its strength. With the use of the SEM and FTIR, the formation and growth of the C-S-H have been examined from 3 to 56 days. On the other hand, with the use of the Forney and MTS testing equipment, the compressive strength of the hardened cement pastes was determined. From the experimental results obtained, several conclusions have been drawn:

1. The presence of nano-silica causes pozzolanic reaction of silica with the calcium hydroxide (CH) which forms more C-S-H-gel and the reduction in the calcium hydroxide.

2. There is an increase in formation of C-S-H with time; signifying the increase in strength over the course of the hydration phases.

3. The addition of nano silica significantly improved the compressive strength of the hardened cement paste tested at different ages. The results indicated that the best improvement in compressive strength was with 1% nano-silica by volume, optimal percentage, followed closely by the 3% NS. The compressive strength of specimens containing 5%

_____

NS portrayed a decrease in strength in comparison to that of the 1% and 3% additions.

4. Water curing proved to be the beneficial form of curing by displaying higher strength values than that of the vacuum cured method. However, the SEM and FTIR studies show identical results for both curing methods.

References

[1] García-Maté, M., De la Torre, A., León-Reina, L., Aranda, M., Santacruz, I.: *Hydration Studies of Calcium Sulfoaluminate Cements Blended with Fly Ash*, Cement and Concrete Research, 54 (2013), 12-20.

[2] Zhang, Y. M. et al.: *Hydration of High-Volume Fly Ash Cement Paste*, Cement and Cement Paste Composites, (2000), 445-452.

[3] Bagheri, A., Zanganeh, H., Alizaden, H., Shakerinian, M., Marian, M.: *Comparing the performance of fly ash and silica fume in enhancing the properties of concrete containing fly-ash*, Construction, and Building Materials, 47 (2013), 1402-1408.

[4] Björnström, J., Martinelli, A., Matic, A., Börjesson L., Panas, I.: *Accelerating effects of colloidal Nano-Silicafor beneficial calcium–silicate–hydrate formation in cement*, Chemical Physics Letters 392 (2004), 1-3, 242-248.

[5] Jonbi, Pane, I., Hariandja, B., Imran, I.: *The Use of Nano silica for Improving Concrete Compressive Strength and Durability*, Applied Mechanics and Materials, (2012), 4059-4062.

[6] Sobolev, K., Flores, I., Torres-Martinez, L. M, Valdez, P. L., Zarazua, P. L., Cuellar, E. L.: *Engineering of SiO2 nanoparticles for optimal performance in nano cement-based materials*, In Nanotechnology in Construction, 3 (2009), 5, 139-148.

[7] Maheswaran, S., Bhuvaneshwari, B., Palani, G. S., Nagesh R., Kalaiselvam, S.: *An Overview on the Influence of Nano-Silica in Concrete and a Research Initiative*, Research Journal of Recent Sciences 2, (2013), 17-24.

[8] Qing, Y., Zenan, Z., Deyu, K., Rongshen, C.: *Influence of nano-SiO2 addition on properties of hardened cement paste as compared with silica fume*, Construction and Building Materials, 21 (2007), 539-545.

[9] Cheuny, J., Jeknavoria, A., Roberts, L. , Silva, D., *Impact of admixtures of the hydration kinetics of Portland cement*, Cement and Concrete Research, 1 (2011), 41, 1289-1309.

[10] ASTM C109 / C109M - 16a (2016), Standard Test Method for Compressive Strength of Hydraulic Cement Mortars (Using 2-in. or [50-mm] Cube Specimens).

[11] ASTM C39 / C39M - 17a (2017), Standard Test Method for Compressive Strength of Cylindrical Concrete Specimens.

[12] Ylmén, R., Jäglid, U., Steenari, B. M., Panas, I.: *Early hydration and setting of Portland cement monitored by IR, SEM and Vicat techniques*, Cement and Concrete Research, 39 (2009), 5, 433-439.

[13] Aversa, R., Petrescu, R. V., Apicella, A., Petrescu, F. I.: *Nano-Diamond Hybrid Materials for Structural Biomedical Application*, American Journal of Biochemistry and Biotechnology, 13, (2017), 34-41.

[14] Syed, J., Dharrab, A., Zafa, M.S., Khand, E., Aversa, R., Petrescu, R. V., Apicella, A., Petrescu, F. I.: *Influence of Curing Light Type and Staining Medium on the Discoloring Stability of Dental Restorative Composite*, American Journal of Biochemistry and Biotechnology, 13 (2017), 1, 42-50.

[15] Aversa, R., Parcesepe, D., Petrescu, R. V., Berto, F., Chen, G., Petrescu, F. I., Tamburrino, F., Apicella, A.: *Processability of Bulk Metallic Glasses*, American Journal of Applied Sciences, 14 (2017), 2, 294-301.

[16] Petrescu, R. V., Aversa, R., Akash, B., Bucinell, R., Corchado, J., Berto, F., Mirsayar, M. M., Kosaitis, S., Abu-Lebdeh, T., Apicella, A., Petrescu, F.I.: *Testing by Non-Destructive Control*, American Journal of Engineering and Applied Sciences, 10 (2017), 2, 568-583.

[17] Mirsayar, M. M., Joneidi, V. A., Petrescu, R. V. V., Petrescu, F. I., Berto, F.: *Extended MTSN criterion for fracture analysis of soda lime glass*, Engineering Fracture Mechanics, (2017) 178, 50–59.

[18] Aversa, R., Parcesepe, D., Petrescu, R. V., Chen, G., Petrescu, F. I., Tamburrino, F., Apicella, A.: *Glassy Amorphous Metal Injection Molded Induced Morphological Defects*, American Journal of Applied Sciences, 13 (2016), 12, 1476-1482.

[19] Aversa, R., Petrescu, R. V., Petrescu, F. I., Apicella, A.: *Smart-Factory: Optimization and Process Control of Composite Centrifuged Pipes*, American Journal of Applied Sciences, 13 (2016), 11, 1330-1341.

[20] Petrescu, R. V., Aversa, R., Apicella, A., Li, S.,

Chen, G., Mirsayar, M. M., Petrescu, F. I.: *Something about Electron Dimension*, American Journal of Applied Sciences, 13 (2016), 11,1272-1276.

[21] Aversa, R., Tamburrino, F., Petrescu, R. V., Petrescu, F. T., Artur, M., Chen, G., Apicella, A.: *Biomechanically Inspired Shape Memory Effect Machines Driven by Muscle like Acting NiTi Alloys*, American Journal of Applied Sciences, 13 (2016), 11, 1264-1271.

[22] Petrescu, F. I., Apicella, A., Aversa R., Petrescu, R. V., Calautit, J. K., Mirsayar, M. M., Riccio, A.: *Something about the Mechanical Moment of Inertia*, American Journal of Applied Sciences, 13 (2016), 11, 1085-1090.

[23] Petrescu, F. I., Calautit, J. K.: *About Nano Fusion and Dynamic Fusion*, American Journal of Applied Sciences, 13 (2016), 3, 261-266.

[24] Aversa, R., Petrescu, F. I., Petrescu, R. V., Apicella, A.: *Biofidel FEA Modeling of Customized Hybrid Biological Hip Joint Design Part II*, Flexible Stem Trabecular Prostheses, American Journal of Biochemistry and Biotechnology, 12 (2016), 4, 277-285.

[25] Aversa, R., Petrescu, R. V., Sorrentino, R., Petrescu, F.I., Apicella, A.: *Hybrid Ceramo-Polymeric Nanocomposite for Biomimetic Scaffolds Design and Preparation*, American Journal of Engineering and Applied Sciences, 9 (2016), 4, 1096-1105.

[26] Aversa, R., Petrescu, R. V., Petrescu, F. I., Apicella, A.: *Biomimetic and Evolutionary Design Driven Innovation in Sustainable Products Development*, American Journal of Engineering and Applied Sciences, 9 (2016), 4, 1027-1036.

[27] Aversa R., Petrescu, R. V., Apicella A., Petrescu, F. T.: *Physiologic Human Fluids and Swelling Behavior of Hydrophilic Biocompatible Hybrid Ceramo-Polymeric Materials*, American Journal of Engineering and Applied Sciences, 9 (2016), 4, 962-972.

[28] Berto, F., Gagani, A., Aversa, R., Petrescu, R. V., Apicella, A., Petrescu, F. I.: *Multiaxial Fatigue Strength to Notched specimens made of 40CrMoV13.9*, American Journal of Engineering and Applied Sciences, 9 (2016), 4, 1269-1291.